

^{208}Pb -daughter cluster radioactivity and the deformations and orientations of nuclei

Sham K. Arun and Raj K. Gupta

Department of Physics, Panjab University, Chandigarh 160 014, India

BirBikram Singh, Shefali Kanwar, and Manoj K. Sharma

School of Physics and Materials Science, Thapar University, Patiala 147 004, India

(Received 4 May 2009; published 25 June 2009)

The role of deformations and orientations of nuclei is studied for the first time in cluster decays of various radioactive nuclei, particularly those decaying to doubly closed shell, spherical ^{208}Pb daughter nucleus. Also, the significance of using the correct Q -value of the decay process is pointed out. The model used is the preformed cluster model (PCM) of Gupta and collaborators [R. K. Gupta *et al.*, *Proc. Int. Conf. on Nuclear Reactions Mechanisms*, Varenna, 1988, p. 416; *Phys. Rev. C* **39**, 1992 (1989); **55**, 218 (1997); *Heavy Elements and Related New Phenomena*, edited by W. Greiner and R. K. Gupta, World Sc. 1999, Vol. II, p. 731]. In this model, cluster emission is treated as a tunneling of the confining interaction barrier by a cluster considered already preformed with a relative probability P_0 . Since both the scattering potential and potential energy surface due to the fragmentation process in the ground state of the parent nucleus change significantly with the inclusion of deformation and orientation effects, both the penetrability P and preformation probability P_0 of clusters change accordingly. The calculated decay half-lives for all the cluster decays investigated here are generally in good agreement with measured values for the calculation performed with quadrupole deformations β_2 alone and “optimum” orientations of cold elongated configurations. In some cases, particularly for ^{14}C decay of Ra nuclei, the inclusion of multipole deformations up to hexadecapole β_4 is found to be essential for a comparison with data. However, the available β_4 -values, particularly for nuclei in the mass region $16 \leq A \leq 26$, need be used with caution.

DOI: [10.1103/PhysRevC.79.064616](https://doi.org/10.1103/PhysRevC.79.064616)

PACS number(s): 23.60.+e, 23.70.+j, 21.10.Tg, 21.60.Gx

I. INTRODUCTION

Cluster radioactivity is the spontaneous emission of nuclei, heavier than α -particle, from heavy radioactive nuclei and is an established phenomenon since its theoretical prediction in early 1980 [1] and experimental confirmation in 1984 [2]. The ground-state cluster decays of different parent nuclei in the trans-lead region have been observed by many experimental groups around the world, specifically, the clusters ^{14}C , $^{18,20}\text{O}$, ^{23}F , $^{22,24,26}\text{Ne}$, $^{28,30}\text{Mg}$, ^{32}Si , and ^{34}Si , respectively, from $^{221-224,226}\text{Ra}$, $^{226,228}\text{Th}$, ^{231}Pa , $^{230,232,234}\text{U}$, $^{236,238}\text{Pu}$, ^{238}Pu , and ^{242}Cm parents [3,4]. Also, ^{14}C decay from ^{221}Fr and ^{225}Ac , and, more recently ^{14}C from ^{223}Ac and ^{34}Si from ^{238}U are observed [5]. It is now well understood that these decays find their origin in the closed shell effects of daughter nuclei (^{208}Pb or its neighboring nuclei), studied on various theoretical models, classified mainly as the “fission models” and the “preformed cluster models” (see, e.g., [4]). The shell structure of the daughter nucleus or the Q -value [$\text{B.E.}_{\text{parent}} - (\text{B.E.}_{\text{daughter}} + \text{B.E.}_{\text{cluster}})$] of the reaction is the key factor in the cluster decay process.

In the present work, we investigate the role of deformation and orientation of the decaying parent nucleus and of emitted fragment(s) in the ground-state decay of the daughter nucleus (nuclei), using the preformed cluster model (PCM) of Gupta and collaborators [6–9]. The study is confined to only those clusters in which the daughter formed is always a ^{208}Pb (doubly closed-shell spherical nucleus with $Z = 82$, $N = 126$) and, in some cases, its heavier isotopes. It is relevant to mention here that all the parents $^{221-224,226}\text{Ra}$, $^{226,228}\text{Th}$, ^{231}Pa , $^{230,232,234}\text{U}$,

$^{236,238}\text{Pu}$, and ^{242}Cm and their respective emitted clusters ^{14}C , $^{18,20}\text{O}$, ^{23}F , $^{22,24,26}\text{Ne}$, $^{28,30}\text{Mg}$, and ^{34}Si considered here are deformed, except for ^{26}Ne and ^{34}Si which are spherical. Also all parent nuclei are prolate deformed whereas clusters ^{14}C , ^{23}F , ^{24}Ne , and ^{30}Mg are oblate deformed and $^{18,20}\text{O}$, ^{22}Ne , and ^{28}Mg are prolate deformed. Another point of interest to note may be that all the parent nuclei, with ^{208}Pb as the daughter product, have almost the same N/Z ratio. The experimental data on cluster decay half-lives for all the chosen cases here are given in Refs. [3,4].

With in the “fission models” of cluster radioactivity, the ground-state deformation effects of the parent and/or daughter, keeping the emitted cluster still spherical, were introduced by Shanmugam and Kamalaharan [10] for the finite-range Yukawa-plus-exponential potential, and for the emitted quadrupole deformed cluster, treating the daughter as spherical, by Gupta *et al.* [11,12] using the double folded Michigan-3 Yukawa (M3Y) potential. The deformation effects of the daughter nucleus, as well as the higher multipole deformations, were also accounted for later with in the M3Y potential [13]. However, for the “preformed cluster models,” both deformation and orientation effects of the parent as well as of decay products are studied only recently with in the PCM of Gupta and collaborators, and only brief reports are made at the conferences [14–16]. The details of this work are published here for the first time. Note that in PCM, not only the shapes of parent, daughter and cluster are important, but also the shapes of all other possible fragmentations of the decaying parent nucleus are important via the calculation of the fragmentation potential, and hence the preformation factor P_0 . We shall

see that the inclusion of deformation and orientation effects of the decaying products change the fragmentation potential energy surface (PES) quite significantly. As a consequence, the relative preformation probabilities P_0 for all the fragments change in the ground-state decay of parent nucleus. Similarly, the scattering potential (barrier position as well as its height) is also modified with deformation and orientation effects of outgoing fragments included, thereby affecting the tunneling through barrier, and hence the penetrability P .

Sections II and III give, respectively, the details of preformed cluster model (PCM) and our calculations for ground-state decays of the chosen parent nuclei. For the ground state binding energies and deformation parameters of nuclei, we use the tables of Möller *et al.* [17]. The nuclei are considered to have the “optimum” orientations for the cold ground-state decay process, i.e., the deformed cluster and daughter nuclei are in an elongated, noncompact configuration of Ref. [18], denoted θ_i^{opt} . Finally, the results are summarized in Sec. IV.

II. THE PREFORMED CLUSTER MODEL (PCM)

The preformed cluster model (PCM) of Gupta and collaborators [6–9], with effects of deformation and orientation degrees of freedom included, is based on the well-known quantum mechanical fragmentation theory (QMFT) [18–20]. In PCM, the clusters are considered to be preborn in the parent nucleus before penetrating the interaction barrier. The model is worked out in term of only one parameter, the neck-length parameter ΔR , assimilating the neck formation effects of the two-centre shell-model shape. The decay constant and hence the decay half-life time in PCM is defined as

$$\lambda = \nu_0 P_0 P, \quad T_{1/2} = \frac{\ln 2}{\lambda}. \quad (1)$$

Here ν_0 is the impinging frequency with which the cluster hits the barrier, given by

$$\nu_0 = \frac{v}{R_0} = \frac{(2E_2/\mu)^{1/2}}{R_0}, \quad (2)$$

where R_0 is the radius of parent nucleus and $E_2 = \frac{1}{2}\mu v^2$ is the kinetic energy of the emitted cluster. The impinging frequency ν_0 is nearly constant $\sim 10^{21} \text{ s}^{-1}$ for all the observed cluster decays. Since both the emitted cluster and daughter nuclei are produced in ground state, the entire positive Q -value of decay is the total kinetic energy, ($Q = E_1 + E_2$), available for the decay process, which is shared between the two fragments, such that for the emitted cluster,

$$E_2 = \frac{A_1}{A} Q \quad (3)$$

and, $E_1 (= Q - E_2)$ is the recoil energy of daughter nucleus. P_0 is preformation probability of the cluster, and P is the WKB penetration probability of the cluster through the barrier, calculated within the QMFT.

The QMFT is worked out in terms of the collective coordinates of mass and charge asymmetries

$$\eta = \frac{A_1 - A_2}{A_1 + A_2} \quad \text{and} \quad \eta_Z = \frac{Z_1 - Z_2}{Z_1 + Z_2},$$

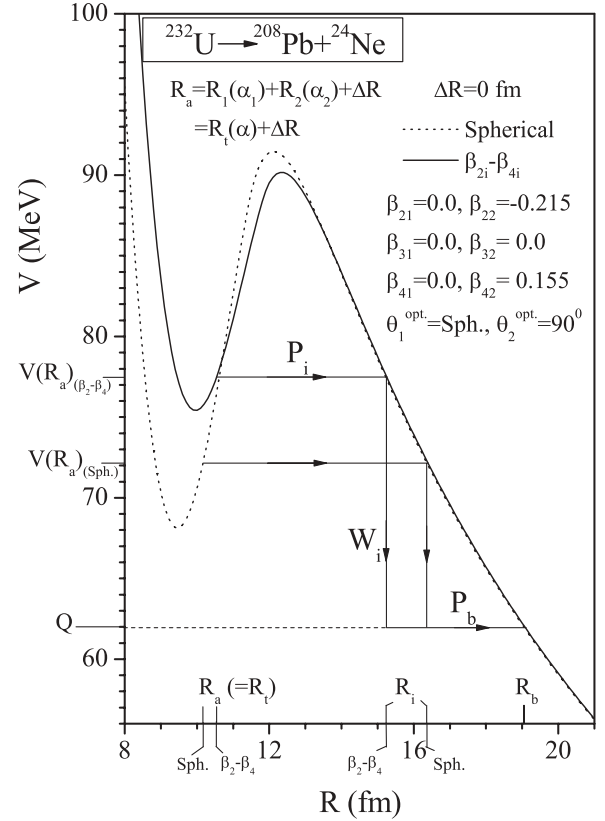


FIG. 1. The scattering potentials for the ^{24}Ne cluster decay of parent nucleus ^{232}U , i.e., $^{232}\text{U} \rightarrow ^{208}\text{Pb} + ^{24}\text{Ne}$, for ^{24}Ne considered as a spherical and deformed nucleus with “optimum” cold orientation angles θ_i^{opt} of Table I in Ref. [18].

(1 and 2 stand, respectively, for the daughter and cluster) and the relative separation R , to which are added the multipole deformations $\beta_{\lambda i}$ and orientations θ_i ($i = 1, 2$) of daughter and cluster nuclei. In PCM, the two coordinates η and R refer, respectively, to the nucleon division (or exchange) between the daughter and cluster, and the transfer of positive Q -value to the total kinetic energy ($E_1 + E_2$) of two nuclei as they are produced in the ground state, as already pointed out above.

The preformation probability $P_0(A_i) = |\psi(\eta(A_i))|^2$, $i = 1$ or 2) is the solution of the stationary Schrödinger equation in η , at fixed $R = R_a$, the first turning point of the penetration path used for calculating the penetrability P (see Fig. 1). Thus, the structure information of the compound nucleus is contained in P_0 via the fragmentation potential,

$$V_R(\eta) = - \sum_{i=1}^2 [B_i(A_i, Z_i)] + V_c(R, Z_i, \beta_{\lambda i}, \theta_i) + V_P(R, A_i, \beta_{\lambda i}, \theta_i) + V_\ell(R, A_i, \beta_{\lambda i}, \theta_i), \quad (4)$$

used in the above said stationary Schrödinger equation. Here, $B_i(A_i, Z_i)$ are the ground state binding energies from Ref. [17], and V_c , V_P , and V_ℓ are, respectively, the Coulomb, nuclear proximity, and angular-momentum dependent potentials. For ground-state decays, $\ell = 0$ is a good approximation [4].

In Eq. (4), the proximity potential V_P for deformed and oriented nuclei (see Figure 2 of [21]) is given as

$$V_P(s_0) = 4\pi \bar{R} \gamma b \Phi(s_0), \quad (5)$$

with the specific nuclear surface tension coefficient $\gamma = 0.9517[1 - 1.7826(\frac{N-Z}{A})^2]$ MeV fm⁻², the surface thickness $b = 0.99$ fm, and the universal function, independent of the geometry of nuclear system, is

$$\Phi(s_0) = \begin{cases} -\frac{1}{2}(s_0 - 2.54)^2 - 0.0852(s_0 - 2.54)^3 \\ -3.437 \exp\left(-\frac{s_0}{0.75}\right), \end{cases} \quad (6)$$

respectively, for $s_0 \leq 1.2511$ and ≥ 1.2511 . Here, s_0 is in units of surface thickness b . For determining the shortest distance s_0 between any two colliding nuclei, we use the expression of Gupta *et al.* [21], obtained for all possible orientations of two equal or unequal, axially symmetric, deformed nuclei lying in one plane (Figure 2 of [21]),

$$s_0 = R - X_1 - X_2, \quad (7)$$

where

$$X_1 = R_1(\alpha_1) \cos(\theta_1 - \alpha_1) \quad (8)$$

and

$$X_2 = R_2(\alpha_2) \cos(180 + \theta_2 - \alpha_2) \quad (9)$$

are the projections along the collision Z-axis of nuclei. The mean curvature radius \bar{R} in Eq. (5) for two co-planer nuclei is

$$\frac{1}{\bar{R}^2} = \frac{1}{R_{11}R_{12}} + \frac{1}{R_{21}R_{22}} + \frac{1}{R_{11}R_{22}} + \frac{1}{R_{21}R_{12}} \quad (10)$$

with the four principal radii of curvature R_{i1} and R_{i2} of the two reaction partners given by Eq. (4) of [21], and the radius vectors

$$R_i(\alpha_i) = R_{0i} \left[1 + \sum_{\lambda} \beta_{\lambda i} Y_{\lambda}^{(0)}(\alpha_i) \right] \quad (11)$$

with the R_{0i} given by

$$R_{0i} = 1.28A_i^{1/3} - 0.76 + 0.8A_i^{-1/3}. \quad (12)$$

For Coulomb interaction, the extended Wong's [22] expression for two non-overlapping charge distributions, to all higher multipole deformations ($\lambda = 2, 3, 4, \dots$), is [18]

$$V_c = \frac{Z_1 Z_2 e^2}{R} + 3Z_1 Z_2 e^2 \sum_{\lambda, i=1,2} \frac{R_i^{\lambda}(\alpha_i)}{(2\lambda + 1)R^{\lambda+1}} \times Y_{\lambda}^{(0)}(\theta_i) \left[\beta_{\lambda i} + \frac{4}{7} \beta_{\lambda i}^2 Y_{\lambda}^{(0)}(\theta_i) \right]. \quad (13)$$

The mass parameters $B_{\eta\eta}(\eta)$, entering the P_0 calculation via the kinetic energy term, are the smooth classical hydrodynamical masses [23], used for reasons of simplicity.

The penetrability P in Eq. (1) is the WKB integral between R_a and R_b , the first and second turning points, respectively (Fig. 1). In other words, the tunneling begins at $R = R_a$ and terminates at $R = R_b$, with $V(R_b) = Q$ -value for ground state decay. Thus, as per Fig. 1, the transmission probability P consists of the following three contributions [6,7]:

(i) The penetrability P_i from R_a to R_i ,

(ii) the (inner) de-excitation probability W_i at R_i , and

(iii) the penetrability P_b from R_i to R_b

giving the penetration probability as

$$P = P_i W_i P_b. \quad (14)$$

The shifting of first turning point from R_a to R_0 , the compound nucleus radius, gives the penetrability P similar to that of Shi and Swiatecki [24] for spherical nuclei, which is known not to fit the experimental data without the adjustment of assault frequency ν_0 . Following the excitation model of Greiner and Scheid [25], we take the de-excitation probability $W_i=1$ for a heavy cluster decays, which reduces Eq. (14) to the following:

$$P = P_i P_b, \quad (15)$$

where P_i and P_b in the WKB approximation are

$$P_i = \exp \left[-\frac{2}{\hbar} \int_{R_a}^{R_i} \{2\mu[V(R) - V(R_i)]\}^{1/2} dR \right] \quad (16)$$

and

$$P_b = \exp \left[-\frac{2}{\hbar} \int_{R_i}^{R_b} \{2\mu[V(R) - Q]\}^{1/2} dR \right]. \quad (17)$$

For the first turning point, we use the following postulate:

$$R_a(\eta) = R_1(\alpha_1) + R_2(\alpha_2) + \Delta R = R_i(\alpha, \eta) + \Delta R, \quad (18)$$

where the η -dependence of R_a is contained in R_i , and ΔR is a parameter, assimilating the neck formation effects of two center shell model [8]. This method of introducing the neck-length parameter ΔR is also used in our dynamical cluster-decay model (DCM) [26–38] and in the scission-point [39] and saddle-point [40,41] (statistical) fission models for decay of a hot and rotating compound nucleus.

III. CALCULATIONS AND DISCUSSION OF THE RESULTS

The scattering potentials in Fig. 1, plotted for the cases of both spherical and deformed nuclei, show that the barrier position as well as height get modified with the inclusion of deformation and orientation effects of the ²⁴Ne cluster. As expected, due to deformations, the barrier height gets reduced and position increased, thereby affecting the tunneling penetrability P . Note that the calculated decay constant λ (or half-life $T_{1/2}$) depends on P , and hence on inclusion/ or noninclusion of deformations and orientations of nuclei.

Another quantity of interest for the calculations of λ or $T_{1/2}$ is the preformation factor P_0 , whose calculation depends on the fragmentation potential $V(A_2)$, illustrated in Fig. 2 for two parent nuclei ²²²Ra and ²³²U. Here we have plotted the cases of spherical vs quadrupole deformations β_2 alone [panel (a)], and β_2 alone vs quadrupole, octupole, hexadecapole deformations (β_2 – β_4) taken into account [panel (b)], for all the possible fragmentations of the parent nucleus. The orientation effects are the ‘‘optimum’’ cold orientation angles θ_i^{opt} of Table I in Ref. [18]. We notice that the inclusion of deformations and orientations of nuclei in $V(A_2)$ change the potential energy surface (PES) significantly, and hence the relative preformation probability P_0 for all the fragments would change accordingly.

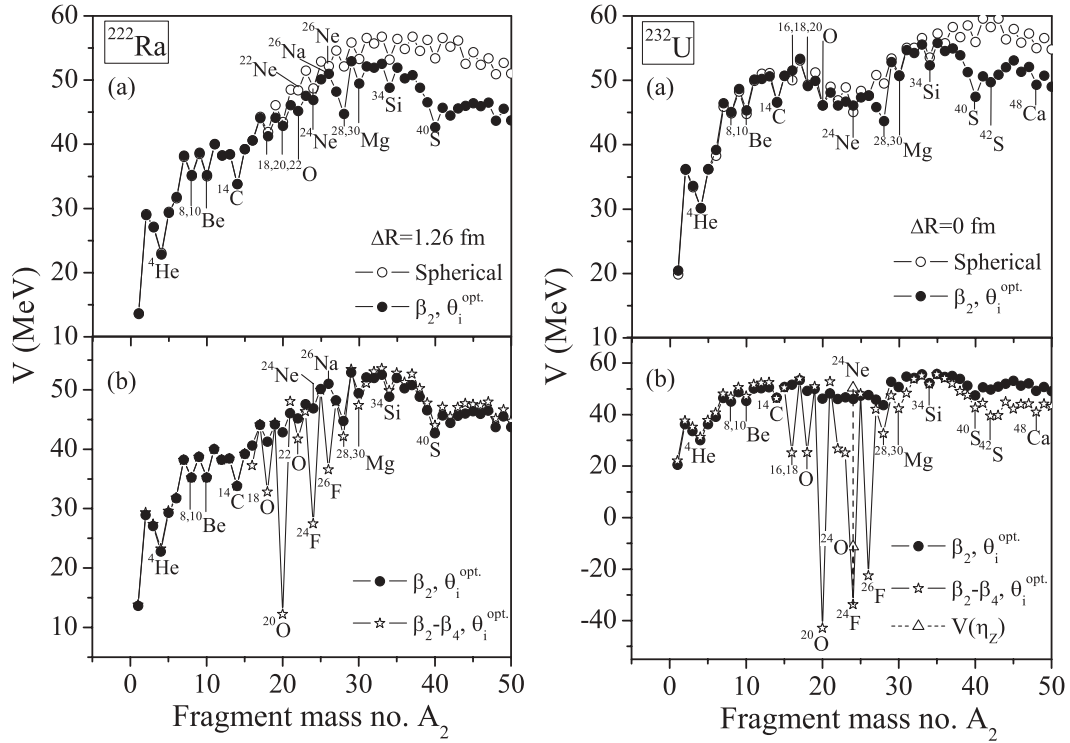


FIG. 2. The fragmentation potentials for parent nuclei ^{222}Ra and ^{232}U , for cases of (a) spherical compared with quadrupole deformation β_2 alone, and (b) quadrupole deformation β_2 alone compared with quadrupole plus octupole plus hexadecapole deformations (β_2 - β_4), taken into account for all possible fragments. The orientation angles are the “optimum” cold θ_i^{opt} of Table I in Ref. [18].

In Fig. 2, we observe that for both the parents, there is no change in PES for the cluster mass up to $A_2 = 15$. For $A_2 > 15$, many new minima are observed in going from spherical to deformed (β_2 alone or β_2 - β_4). For example, in panel (a), new minima at ^{28}Mg and ^{40}S are obtained in going from spherical to β_2 alone, and in the case of including higher multipole deformations ($\beta_2, \beta_3, \beta_4$), many new clusters, like $^{16,18,20}\text{O}$, $^{24,26}\text{F}$, and ^{40}S are favored, which are not experimentally observed, and also get ruled out in calculations because of their small penetrability P . However, the relative

preformation factor P_0 changes considerably, even for lighter clusters of masses $A_2 \leq 15$. This is illustrated in Table I, where both P_0 and P are given for the three cases of spherical, β_2 alone, and ($\beta_2, \beta_3, \beta_4$). Only the experimentally observed clusters with ^{208}Pb -daughter product are considered. Similar remarks are applicable to panel (b), e.g., the observed ^{24}Ne cluster for the parent nucleus ^{232}U is at the minimum only in the spherical case. This is also illustrated for the case of ($\beta_2, \beta_3, \beta_4$) via the charge dispersion potential $V(\eta_z)$ [dashed vertical line in panel (b)], where the minimum is found to lie

TABLE I. The calculated preformation probability P_0 and penetrability P using PCM, for various clusters with ^{208}Pb as the daughter product, for cases of spherical, β_2 alone, and (β_2, β_3 , and β_4) deformed nuclei, and “optimum” orientations.

Parent	Cluster	PCM					
		Preformation probability P_0			Penetration probability P		
		Sph.	β_2	$\beta_2, \beta_3, \beta_4$	Sph.	β_2	$\beta_2, \beta_3, \beta_4$
^{222}Ra	^{14}C	6.54×10^{-22}	1.88×10^{-20}	9.16×10^{-16}	1.55×10^{-18}	1.59×10^{-18}	1.59×10^{-18}
^{226}Th	^{18}O	2.42×10^{-25}	3.59×10^{-23}	9.29×10^{-08}	9.03×10^{-21}	1.13×10^{-20}	
^{228}Th	^{20}O	4.20×10^{-24}	8.44×10^{-23}	9.99×10^{-01}	1.06×10^{-20}	1.12×10^{-20}	
^{231}Pa	^{23}F	3.27×10^{-27}	1.05×10^{-26}	4.13×10^{-09}	1.39×10^{-24}	9.61×10^{-24}	3.06×10^{-23}
^{230}U	^{22}Ne	2.40×10^{-28}	5.61×10^{-23}	8.52×10^{-08}	6.28×10^{-21}	1.48×10^{-19}	1.36×10^{-16}
^{232}U	^{24}Ne	8.64×10^{-26}	1.03×10^{-25}	5.51×10^{-15}	2.38×10^{-21}	2.87×10^{-20}	2.63×10^{-19}
^{234}U	^{26}Ne	3.56×10^{-28}	1.15×10^{-26}	2.52×10^{-16}	6.70×10^{-23}	6.70×10^{-23}	6.70×10^{-23}
^{236}Pu	^{28}Mg	6.56×10^{-28}	6.62×10^{-22}	6.32×10^{-17}	6.92×10^{-20}	2.55×10^{-18}	
^{238}Pu	^{30}Mg	2.74×10^{-28}	3.24×10^{-26}	2.55×10^{-36}	1.42×10^{-19}	9.47×10^{-19}	2.42×10^{-19}
^{242}Cm	^{34}Si	1.14×10^{-27}	1.52×10^{-25}	4.94×10^{-38}	4.85×10^{-19}	4.85×10^{-19}	4.85×10^{-19}

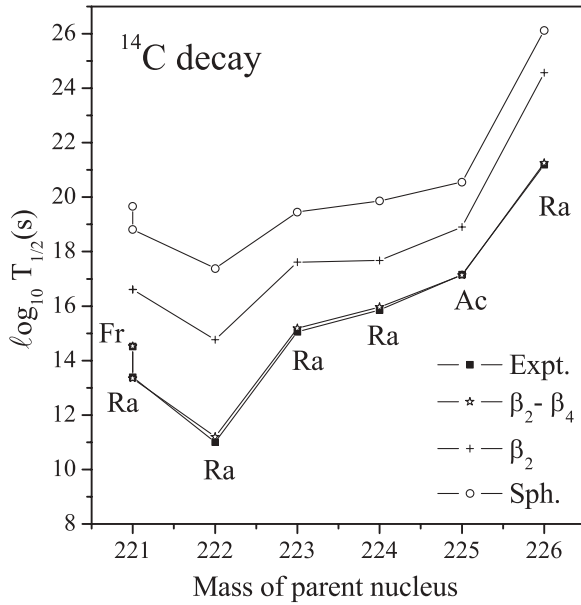


FIG. 3. Comparison between the experimentally observed and calculated decay half-lives for ¹⁴C cluster emitted from various Ra isotopes and ²²¹Fr and ²²⁵Ac parent nuclei in the ground state.

at ²⁴F. Note, however, that both ²⁴F and ²⁴O are prohibited by penetrability *P*. Also, the ²⁸Mg cluster decay of ²³²U, for which only the upper limit of *T*_{1/2} is measured experimentally, becomes more and more favorable as deformation changes from spherical to β_2 , and then to ($\beta_2, \beta_3, \beta_4$) case.

Figure 3 and Table II show the comparison between the experimentally observed cluster decay half-lives and the calculations based on the PCM for the three cases of spherical, quadrupole deformation β_2 alone, and quadrupole, octupole, hexadecapole deformations (β_2, β_3 , and β_4), and “optimum” orientations in each case. Figure 3, for ¹⁴C cluster decay from different Ra isotopes, shows clearly that the comparison

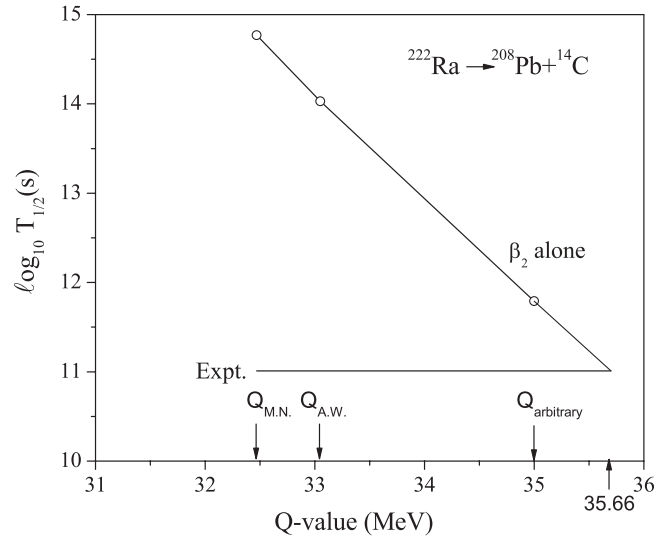


FIG. 4. Comparison between the experimentally observed and calculated half-life for the ¹⁴C cluster emitted from the ²²²Ra as a function of the emitted *Q*-value. The *Q*-values *Q*_{M.N.}, *Q*_{A.W.}, and *Q*_{arbitrary} refer, respectively to Möller *et al.* [17], Audi and Wapstra [42], and an arbitrary value.

between the data and calculations is the best for all considered decays when higher multipole deformations (β_2, β_3 , and β_4) are included. On the other hand, Table II shows that, except for ¹⁴C decay of ²²²Ra (already shown in Fig. 3), the respective cluster decays of all other parent nuclei, i.e., ^{226,228}Th, ²³¹Pa, ^{230,232,234}U, ^{236,238}Pu, and ²⁴²Cm, are best explained for the case of quadrupole deformation β_2 alone. In the case of higher multipole deformations (β_2 – β_4) included, the $\log_{10} T_{1/2}$ is underestimated, possibly due to the inadequate β_4 values calculated in Ref. [17], in particular for the mass region $16 \leq A_2 \leq 26$ (the experimental β_4 values are not available). The only parameter of model is the length parameter ΔR

TABLE II. Half-life times and other characteristic quantities for cluster decay of various parent nuclei. The calculations are made for use of the preformed cluster-decay model (PCM) of Gupta and collaborators, for cases of spherical, β_2 alone and (β_2, β_3 , and β_4) deformed nuclei, and “optimum” orientations. The impinging frequency $\nu_0 \sim 10^{21} \text{ s}^{-1}$ for each case. *Q*_{M.N.} refers to the *Q*-value calculated by using the binding energies of Möller *et al.* [17].

Parent	Cluster	<i>R</i> _a	<i>Q</i> _{M.N.}	PCM			Expt.
				Half-lives $\log_{10} T_{1/2}$			Half-lives
				Sph.	β_2	$\beta_2, \beta_3, \beta_4$	$\log_{10} T_{1/2}$
²²² Ra	¹⁴ C	<i>R</i> _t + 1.26	32.47	17.36	15.89	11.20	11.01
²²⁶ Th	¹⁸ O	<i>R</i> _t	47.55	23.00	20.73		> 15.3
²²⁸ Th	²⁰ O	<i>R</i> _t + 0.50	45.91	21.72	20.40		20.87
²³¹ Pa	²³ F	<i>R</i> _t + 0.25	50.81	28.73	27.38	09.28	> 24.61
²³⁰ U	²² Ne	<i>R</i> _t	61.69	26.15	19.41	01.27	> 18.2
²³² U	²⁴ Ne	<i>R</i> _t	62.03	24.04	22.88	11.19	21.05
²³⁴ U	²⁶ Ne	<i>R</i> _t + 0.50	58.65	28.00	26.49	16.15	25.06
²³⁶ Pu	²⁸ Mg	<i>R</i> _t	78.75	24.68	17.11		21.67
²³⁸ Pu	³⁰ Mg	<i>R</i> _t + 0.50	76.82	24.77	21.87	32.57	25.70
²⁴² Cm	³⁴ Si	<i>R</i> _t	95.78	23.59	21.47	33.96	23.24

whose value is, in general, obtained to be zero or small. In other words, the decay process, in general, occurs near/ or at the touching configuration.

Finally, a few words on the importance of Q -value used in the PCM calculations. Figure 4 shows the variation of calculated decay half-life for ^{14}C decay of ^{222}Ra on the Q -value for the case of quadrupole deformation β_2 alone. Apparently, the $\log_{10} T_{1/2}$ value is different for the Q -value calculated from Audi and Wapstra [42] or Möller *et al.* [17], and shows a steep decrease as the Q -value increases. Hence, a measurement of the Q -value together with the $T_{1/2}$ value in an experiment is very important.

IV. SUMMARY

The role of multipole deformations and orientations of nuclei are included in cluster radioactivity for the first time, and found that both deformations and orientations have significant effects on calculated decay half-lives. The measured data on cluster decay half-lives show, in general, improved fits with calculations on the preformed cluster model (PCM) where the effects of deformations are included up to quadrupole deformation only. However, in some cases (particularly, Ra isotopes) the inclusion of higher multipole deformations (up

to hexadecapole deformation) are found essential for a proper comparison between the experiments and calculations. The interesting point is that both the preformation factor P_0 and penetrability P are shown to get modified with the inclusion of deformation and orientation effects. Moreover, unlike P , the P_0 is affected not only due to the shapes of parent, daughter and cluster nuclei, but also due to the shapes of all other possible fragmentations of the decaying parent nucleus.

The present study clearly points out the importance of deformation and orientation effects in cluster decays of radioactive nuclei. The role of multipole deformations higher than β_2 , however, needs a closer look before reaching at any discrete conclusion since the (calculated) data used so far for β_3 and β_4 may not be adequate. Also, the Q -values, calculated from available binding energies, are shown to be very important for predicting the cluster-decay half-lives.

ACKNOWLEDGMENTS

R.K.G. is thankful to Department of Science and Technology, Government of India, and M.K.S. to the University Grant Commission (UGC), New Delhi, for support of this research work.

-
- [1] A. Săndulescu, D. N. Poenaru, and W. Greiner, *Sov. J. Part. Nuclei* **11**, 528 (1980).
- [2] H. J. Rose and G. A. Jones, *Nature (London)* **307**, 245 (1984).
- [3] R. Bonetti and A. Guglielmetti, in *Heavy Elements and Related New Phenomena*, edited by W. Greiner and R. K. Gupta (World Scientific, Singapore, 1999), Vol. II, p. 643.
- [4] R. K. Gupta and W. Greiner, *Int. J. Mod. Phys. E* **3**, 335 (Suppl., 1994).
- [5] R. Bonetti and A. Guglielmetti, *Romanian Reports in Phys.* **59**, 301 (2007); private communication to one of us (R.K.G.).
- [6] R. K. Gupta, in *Proceedings of the 5th International Conference on Nuclear Reaction Mechanisms*, Varenna, edited by E. Gadioli (Ricerca Scientifica ed Educazione Permanente, Milano, 1988), p. 416.
- [7] S. S. Malik and R. K. Gupta, *Phys. Rev. C* **39**, 1992 (1989).
- [8] S. Kumar and R. K. Gupta, *Phys. Rev. C* **55**, 218 (1997).
- [9] R. K. Gupta, in *Heavy Elements and Related New Phenomena*, edited by W. Greiner and R. K. Gupta (World Scientific, Singapore, 1999), Vol. II, p. 731.
- [10] G. Shanmugam and B. Kamalaharan, *Phys. Rev. C* **41**, 1184 (1990).
- [11] A. Săndulescu, R. K. Gupta, F. Carstoiu, M. Horoi, and W. Greiner, *Int. J. Mod. Phys. E* **1**, 379 (1992).
- [12] R. K. Gupta, M. Horoi, A. Săndulescu, M. Greiner, and W. Scheid, *J. Phys. G: Nucl. Part. Phys.* **19**, 2063 (1993).
- [13] S. Măicu and D. Protopopescu, *Acta Phys. Pol. B* **30**, 127 (1999).
- [14] S. K. Arun and R. K. Gupta, *Proceedings of the Department of Atomic Energy Symposium on Nuclear Physics, 2007*, Vol. 52, p. 365.
- [15] B. B. Singh, S. K. Arun, S. Kanwar, M. K. Sharma, and R. K. Gupta, *Proceedings of the Department of Atomic Energy Symposium on Nuclear Physics, 2008*, Vol. 53, p. 259.
- [16] M. K. Sharma, B. B. Singh, and R. K. Gupta, Contributions to the Punjab Science Congress, Patiala, 2008, p. 40.
- [17] P. Möller, J. R. Nix, W. D. Myers, and W. J. Swiatecki, *At. Data Nucl. Data Tables* **59**, 185 (1995).
- [18] R. K. Gupta, M. Balasubramaniam, R. Kumar, N. Singh, M. Mahhas, and W. Greiner, *J. Phys. G: Nucl. Part. Phys.* **31**, 631 (2005).
- [19] J. Maruhn and W. Greiner, *Phys. Rev. Lett.* **32**, 548 (1974).
- [20] R. K. Gupta, W. Scheid, and W. Greiner, *Phys. Rev. Lett.* **35**, 353 (1975).
- [21] R. K. Gupta, N. Singh, and M. Mahhas, *Phys. Rev. C* **70**, 034608 (2004).
- [22] C. Y. Wong, *Phys. Rev. Lett.* **31**, 766 (1973).
- [23] H. Kröger and W. Scheid, *J. Phys. G* **6**, L85 (1980).
- [24] Y. J. Shi and W. J. Swiatecki, *Phys. Rev. Lett.* **54**, 300 (1985).
- [25] M. Greiner and W. Scheid, *J. Phys. G: Nucl. Part. Phys.* **12**, L229 (1986).
- [26] R. K. Gupta, M. Balasubramaniam, C. Mazzocchi, M. La Commara, and W. Scheid, *Phys. Rev. C* **65**, 024601 (2002).
- [27] R. K. Gupta, R. Kumar, N. K. Dhiman, M. Balasubramaniam, W. Scheid, and C. Beck, *Phys. Rev. C* **68**, 014610 (2003).
- [28] R. K. Gupta, *Acta Phys. Hung. (N. S.) Heavy Ion Phys.* **18**, 347 (2003).
- [29] M. Balasubramaniam, R. Kumar, R. K. Gupta, C. Beck, and W. Scheid, *J. Phys. G: Nucl. Part. Phys.* **29**, 2703 (2003).
- [30] R. K. Gupta, M. Balasubramaniam, R. Kumar, D. Singh, and C. Beck, *Nucl. Phys.* **A738**, 479c (2004).
- [31] R. K. Gupta, M. Balasubramaniam, R. Kumar, D. Singh, C. Beck, and W. Greiner, *Phys. Rev. C* **71**, 014601 (2005).
- [32] R. K. Gupta, M. Balasubramaniam, R. Kumar, D. Singh, S. K. Arun, and W. Greiner, *J. Phys. G: Nucl. Part. Phys.* **32**, 345 (2006).

- [33] B. B. Singh, M. K. Sharma, R. K. Gupta, and W. Greiner, *Int. J. Mod. Phys. E* **15**, 699 (2006).
- [34] B. B. Singh, M. K. Sharma, and R. K. Gupta, *Phys. Rev. C* **77**, 054613 (2008).
- [35] R. K. Gupta, S. K. Arun, D. Singh, R. Kumar, Niyti, S. K. Patra, P. Arumugam, and B. K. Sharma, *Int. J. Mod. Phys. E* **17**, 2244 (2008).
- [36] R. K. Gupta, S. K. Arun, R. Kumar, and Niyti, *Int. Rev. Phys. (IREPHY)* **2**, 369 (2008).
- [37] R. Kumar and R. K. Gupta, *Phys. Rev. C* **79**, 034602 (2009).
- [38] R. K. Gupta, Niyti, M. Manhas, S. Hofmann, and W. Greiner, *Int. J. Mod. Phys. E* **18**, 601 (2009).
- [39] T. Matsuse, C. Beck, R. Nouicer, and D. Mahboub, *Phys. Rev. C* **55**, 1380 (1997).
- [40] S. J. Sanders, D. G. Kovar, B. B. Back, C. Beck, D. J. Henderson, R. V. F. Janssens, T. F. Wang, and B. D. Wilkins, *Phys. Rev. C* **40**, 2091 (1989).
- [41] S. J. Sanders, *Phys. Rev. C* **44**, 2676 (1991).
- [42] G. Audi and A. H. Wapstra, *Nucl. Phys.* **A595**, 409 (1995).